Probabilistic Normal Epipolar Constraint

Dominik Muhle
Technische Universität München
Fakultät für Informatik
Chair of Computer Vision & Artificial Intelligence
München, 23. September 2021

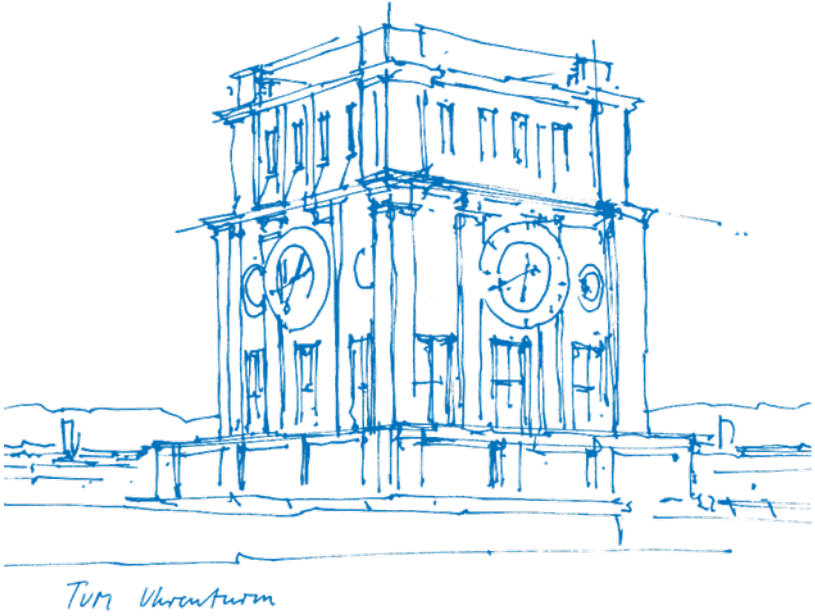

Rotation Estimation under Uncertain Feature Positions

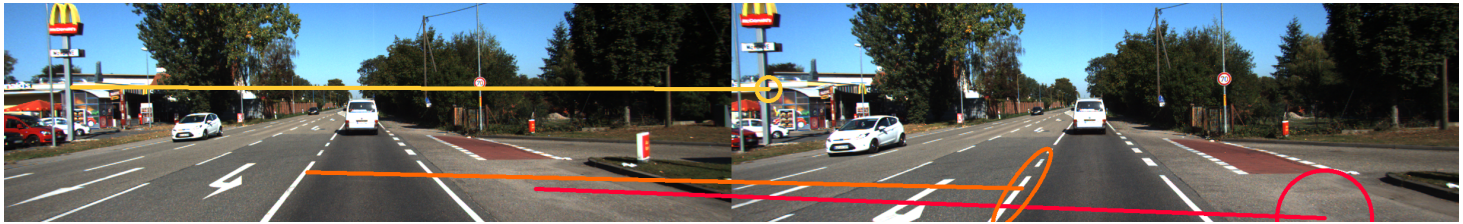

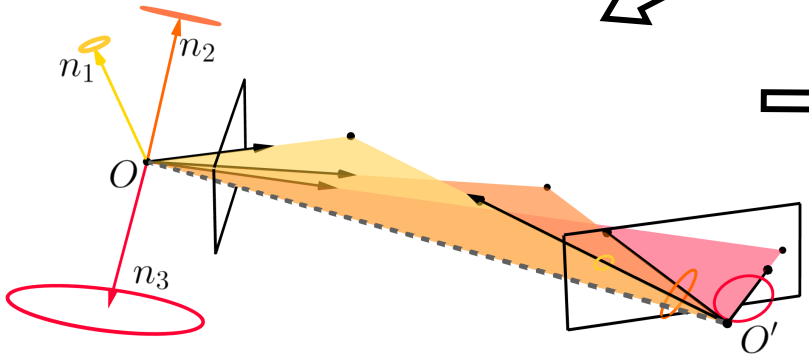

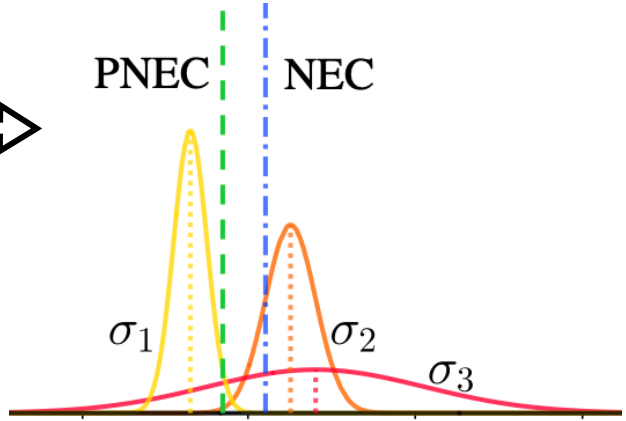

Normal Epipolar Constraint

The normal epipolar constraint (NEC) decouples the rotation from the translation

The NEC is based on the coplanarity of the epipolar plane normal vectors

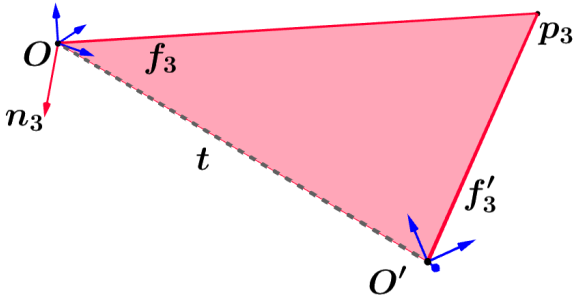

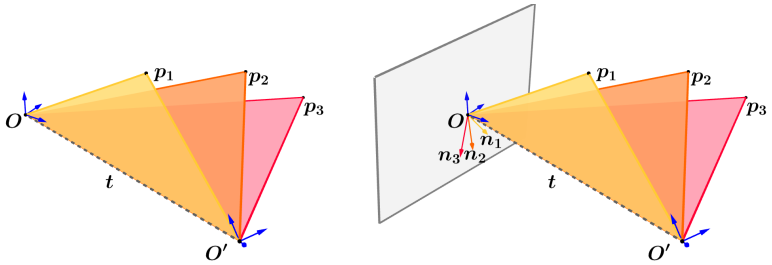

- L. Kneip, R. Siegwart, and M. Pollefeys. Finding the exact rotation between two images independently of the translation. In European Conference on Computer Vision (ECCV), 2012.
- L. Kneip and S. Lynen. Direct optimization of frame-to-frame rotation. In IEEE International Conference on Computer Vision (ICCV), 2013.

Normal Epipolar Constraint

The normal epipolar constraint (NEC) decouples the rotation from the translation

The NEC is based on the coplanarity of the epipolar plane normal vectors

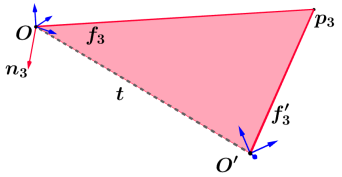

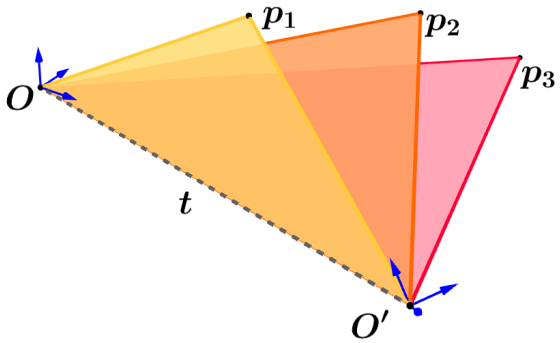

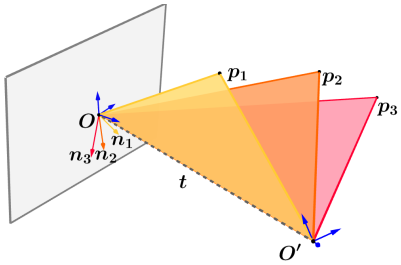

- L. Kneip, R. Siegwart, and M. Pollefeys. Finding the exact rotation between two images independently of the translation. In European Conference on Computer Vision (ECCV), 2012.
- L. Kneip and S. Lynen. Direct optimization of frame-to-frame rotation. In IEEE International Conference on Computer Vision (ICCV), 2013.

Normal Epipolar Constraint

The normal epipolar constraint (NEC) decouples the rotation from the translation

The NEC is based on the coplanarity of the epipolar plane normal vectors

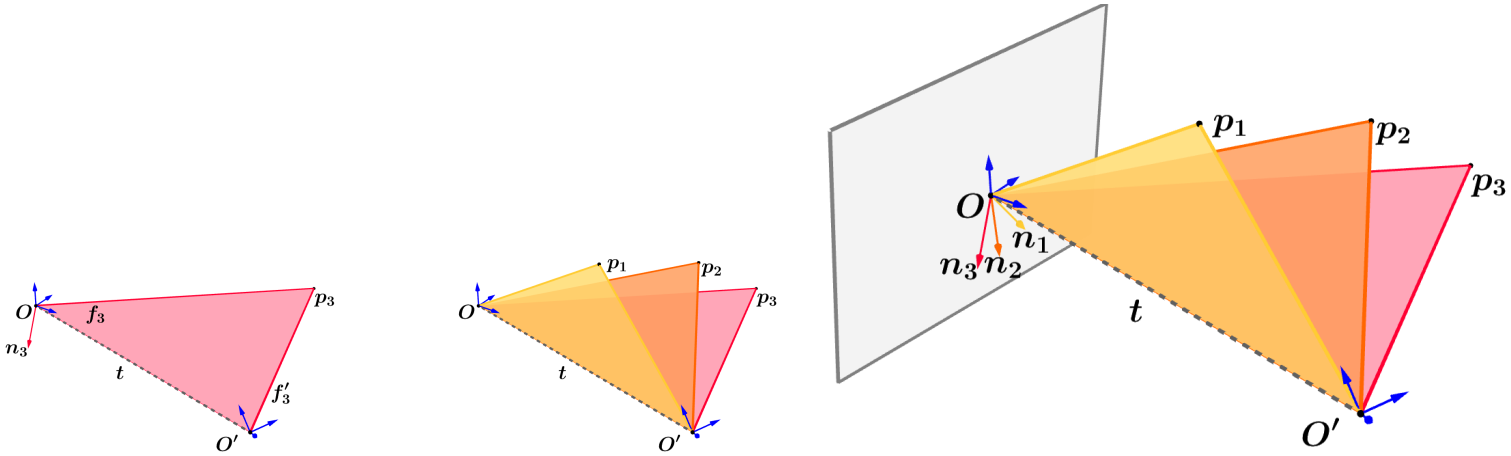

- L. Kneip, R. Siegwart, and M. Pollefeys. Finding the exact rotation between two images independently of the translation. In European Conference on Computer Vision (ECCV), 2012.
- L. Kneip and S. Lynen. Direct optimization of frame-to-frame rotation. In IEEE International Conference on Computer Vision (ICCV), 2013.

Normal Epipolar Constraint

Rotation Estimation

Two camera views

$$\boldsymbol{R} \in SO(3), \boldsymbol{t} \in \mathbb{R}^3 : \|\boldsymbol{t}\| = 1 \tag{1}$$

The normal vector

$$\boldsymbol{n}_i = \boldsymbol{f}_i \times \boldsymbol{R}\boldsymbol{f}'_i \tag{2}$$

For rotation estimation $\boldsymbol{n}_i$ is not in the *epipolar normal plane*

$$e_i = |\boldsymbol{t}^\top \boldsymbol{n}_i| \tag{3}$$

$\rightarrow$ Optimization problem

$$E(\boldsymbol{R}, \boldsymbol{t}) = \sum_i e_i^2 = \sum_i |\boldsymbol{t}^\top \boldsymbol{n}_i|^2 \tag{4}$$

$$= \boldsymbol{t}^T \sum_i \boldsymbol{n}_i \boldsymbol{n}_i^T \boldsymbol{t} \tag{5}$$

Normal Epipolar Constraint

Rotation Estimation

The optimization problem is of the quadratic form

$$E(\boldsymbol{R}, \boldsymbol{t}) = \boldsymbol{t}^\top \boldsymbol{M}(\boldsymbol{R})\boldsymbol{t} \tag{6}$$

Reducing it to a rotation estimation without translation

$$\begin{aligned} \min_{\substack{\boldsymbol{R}\in\mathrm{SO}(3)\\ \boldsymbol{t}:\,\|\boldsymbol{t}\|=1}} \boldsymbol{t}^\top \boldsymbol{M}(\boldsymbol{R})\boldsymbol{t} &= \min_{\boldsymbol{R}\in\mathrm{SO}(3)} \boldsymbol{t}^\top \lambda_{\min}(\boldsymbol{M}(\boldsymbol{R}))\boldsymbol{t} \\ &= \min_{\boldsymbol{R}\in\mathrm{SO}(3)} \lambda_{\min}(\boldsymbol{M}(\boldsymbol{R})) \end{aligned} \tag{7}$$

gives an eigenvalue based optimization scheme

- L. Kneip and S. Lynen. Direct optimization of frame-to-frame rotation. In IEEE International Conference on Computer Vision (ICCV), 2013.
- S. Lee and J. Civera. Rotation-only bundle adjustment. In IEEE Conference on Computer Vision and Pattern Recognition (CVPR), 2021.

Probablistic Normal Epipolar Constraint

Incorporate uncertainty into the NEC

Propagate the uncertainty through the energy function

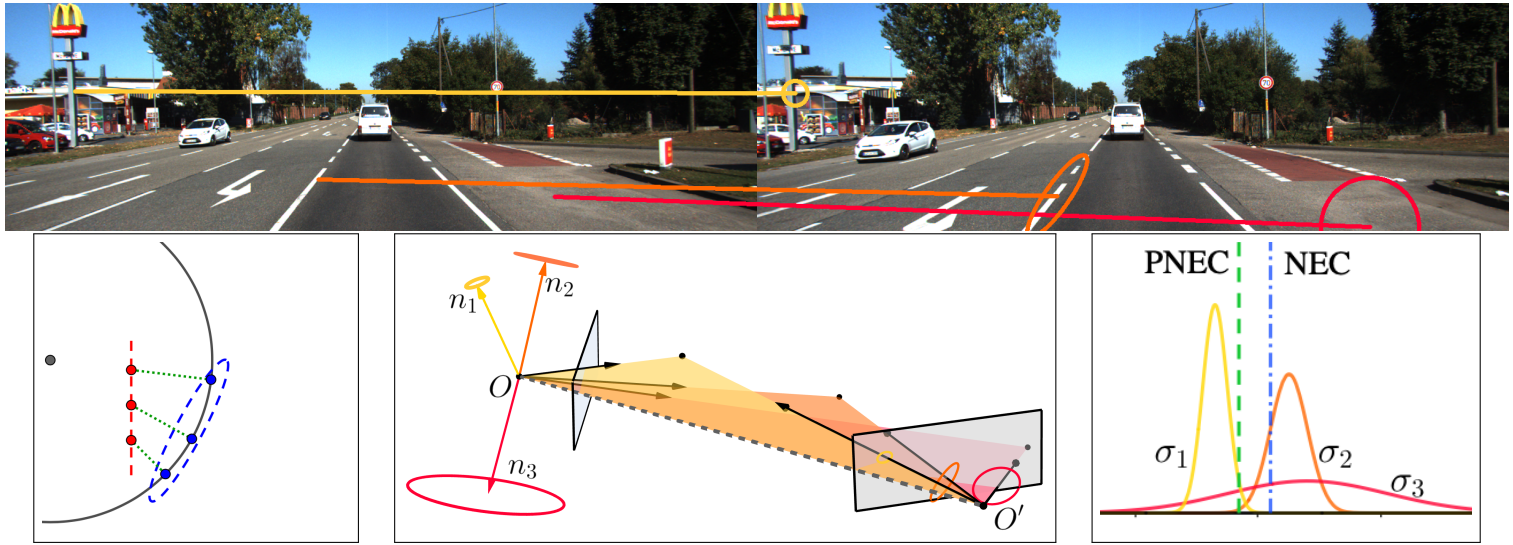

Probabilistic Normal Epipolar Constraint

Energy Function

The propagation of the unit bearing vector covariance $\boldsymbol{\Sigma}_i$ through the linear functions gives a variance of the error term

$$\sigma_i^2 = \boldsymbol{t}^\top \hat{\boldsymbol{f}}_i \boldsymbol{R} \boldsymbol{\Sigma}_i \boldsymbol{R}^\top \hat{\boldsymbol{f}}_i^\top \boldsymbol{t} \tag{8}$$

The weighted optimization function

$$E_P(\boldsymbol{R}, \boldsymbol{t}) = \sum_i \frac{|\boldsymbol{t}^\top \boldsymbol{n}_i|^2}{\sigma_i^2} = \sum_i \frac{\boldsymbol{t}^\top \boldsymbol{n}_i \boldsymbol{n}_i^\top \boldsymbol{t}}{\boldsymbol{t}^\top \hat{\boldsymbol{f}}_i \boldsymbol{R} \boldsymbol{\Sigma}_i \boldsymbol{R}^\top \hat{\boldsymbol{f}}_i^\top \boldsymbol{t}} \tag{9}$$

The alternative form

$$E_P(\boldsymbol{R}, \boldsymbol{t}) = \boldsymbol{t}^\top \sum_i \frac{\boldsymbol{n}_i \boldsymbol{n}_i^\top}{\boldsymbol{t}^\top \hat{\boldsymbol{f}}_i \boldsymbol{R} \boldsymbol{\Sigma}_i \boldsymbol{R}^\top \hat{\boldsymbol{f}}_i^\top \boldsymbol{t}} \boldsymbol{t} \tag{10}$$

Probabilistic Normal Epipolar Constraint

Optimization over $\boldsymbol{t}$

Optimization over the translation is the minimization of a sum of generalized Rayleigh quotients.

$$\min_{\boldsymbol{t}:\,\|\boldsymbol{t}\|=1} E_P(\boldsymbol{t}) = \min_{\boldsymbol{t}:\,\|\boldsymbol{t}\|=1} \sum_i \frac{|\boldsymbol{t}^\top \boldsymbol{n}_i|^2}{\sigma_i^2} = \sum_i \frac{\boldsymbol{t}^\top \boldsymbol{n}_i \boldsymbol{n}_i^\top \boldsymbol{t}}{\boldsymbol{t}^\top \hat{\boldsymbol{f}}_i \boldsymbol{R} \boldsymbol{\Sigma}_i \boldsymbol{R}^\top \hat{\boldsymbol{f}}_i^\top \boldsymbol{t}} \tag{11}$$

No optimal solution is known for this problem.

The self-consistent field algorithm performs better than generic manifold optimization.

- L. Zhang. On optimizing the sum of the rayleigh quotient and the generalized rayleigh quotient on the unit sphere. Computational Optimization and Applications, 54, 2013.

Probabilistic Normal Epipolar Constraint

Optimization over $\boldsymbol{R}$

The rotation estimation cannot be decoupled from the translation

$$\min_{\boldsymbol{R}\in\mathrm{SO}(3)} E_P(\boldsymbol{R}) = \min_{\boldsymbol{R}\in\mathrm{SO}(3)} \boldsymbol{t}^\top \sum_i \frac{\boldsymbol{n}_i \boldsymbol{n}_i^\top}{\boldsymbol{t}^\top \hat{\boldsymbol{f}}_i \boldsymbol{R} \boldsymbol{\Sigma}_i \boldsymbol{R}^\top \hat{\boldsymbol{f}}_i^\top \boldsymbol{t}} \boldsymbol{t} \tag{12}$$

Fixing the weights $\sigma_i'^2 = \sigma_i^2(\boldsymbol{R}_t, \boldsymbol{t}_t)$ allows for the NEC eigenvalue-based optimization

$$\min_{\boldsymbol{R}\in\mathrm{SO}(3)} E_P(\boldsymbol{R}) \approx \min_{\boldsymbol{R}\in\mathrm{SO}(3)} \boldsymbol{t}^\top \sum_i \frac{\boldsymbol{n}_i \boldsymbol{n}_i^\top}{\sigma_i'^2} \boldsymbol{t} = \min_{\boldsymbol{R}\in\mathrm{SO}(3)} \boldsymbol{t}^\top \boldsymbol{M}_P(\boldsymbol{R}) \boldsymbol{t} \tag{13}$$

Probabilistic Normal Epipolar Constraint

Full Optimization

The iterative eigenvalue-based optimization is refined with a least-squares optimization

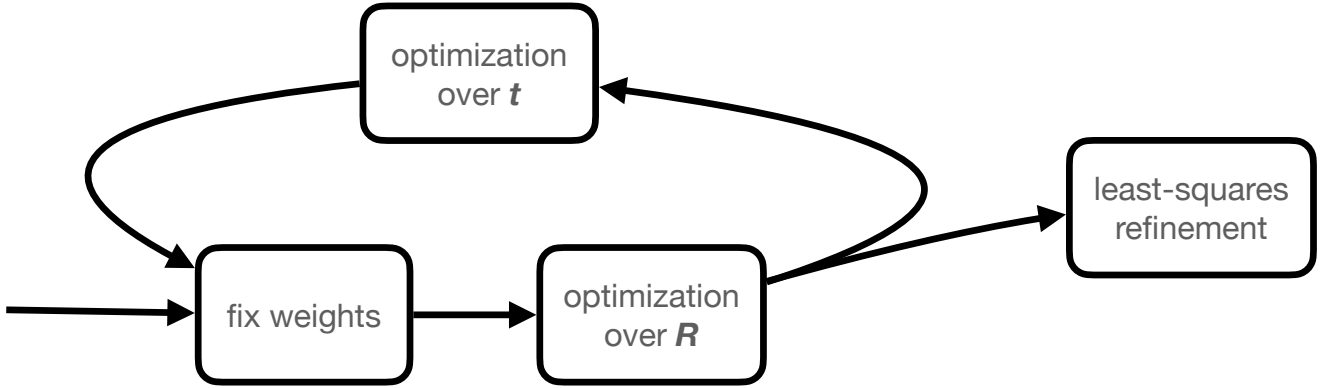

Probabilistic Normal Epipolar Constraint

Singularities

The PNEC energy has a singularity for $\boldsymbol{t} = \boldsymbol{f}_i$

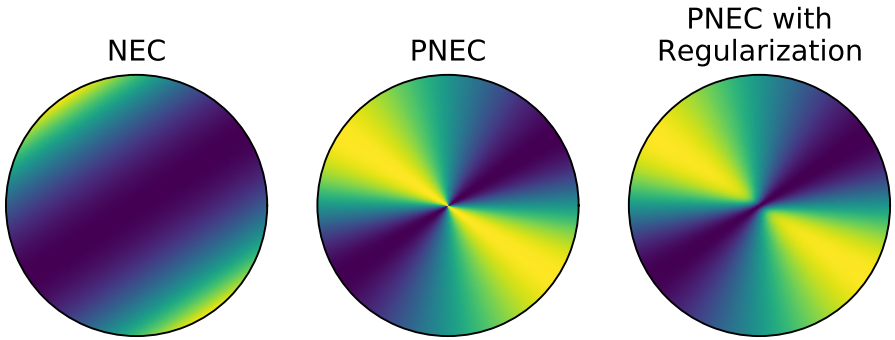

This is removed by considering covariance of the form $\sigma'^2_i = \sigma_i^2 + c$.

Evaluation

Frame-To-Frame Rotation Estimation

Synthetic experiments for omnidirectional cameras

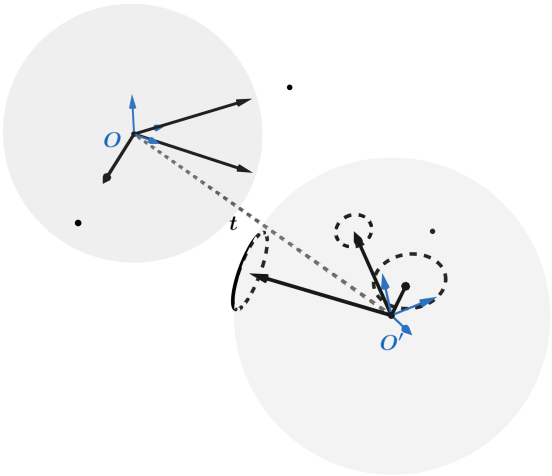

Evaluation

Noise Types

Different noise types

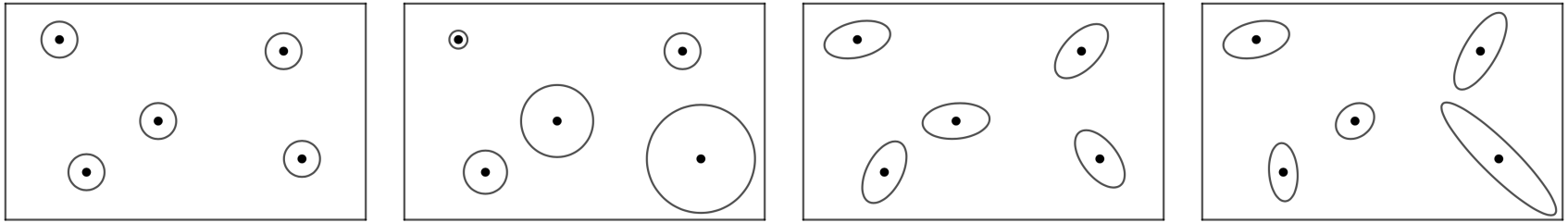

(a) isotropic homogeneous (b) isotropic inhomogeneous (c) anisotropic homogeneous (d) anisotropic inhomogeneous

Evaluation

Frame-To-Frame Rotation Estimation

Frame-to-frame estimation of the PNEC and NEC

For simulated experiments with anisotropic inhomogeneous noise

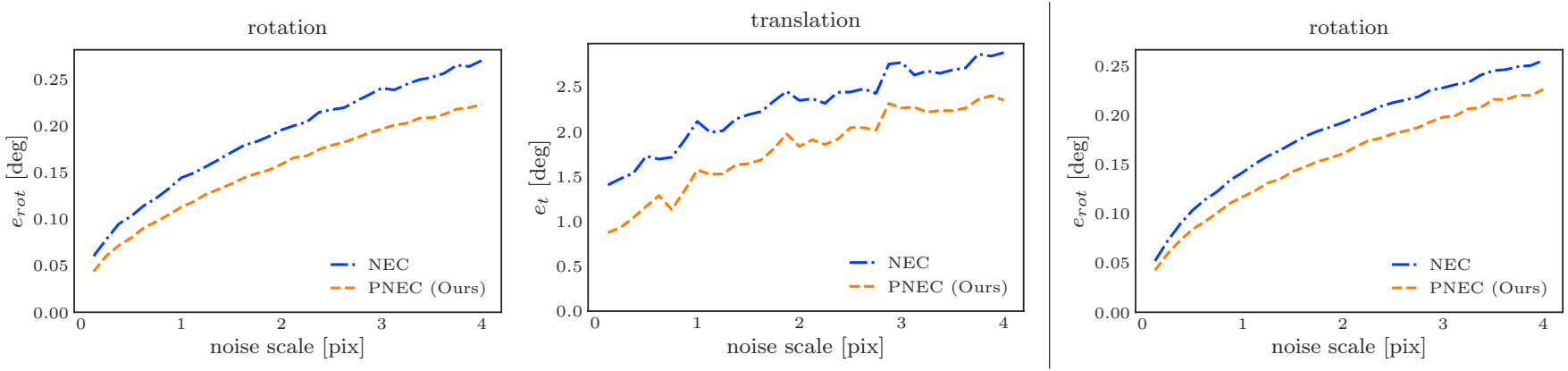

Evaluation

Visual Odometry System

Integration of the PNEC into the rotation only visual odometry algorithm MRO.

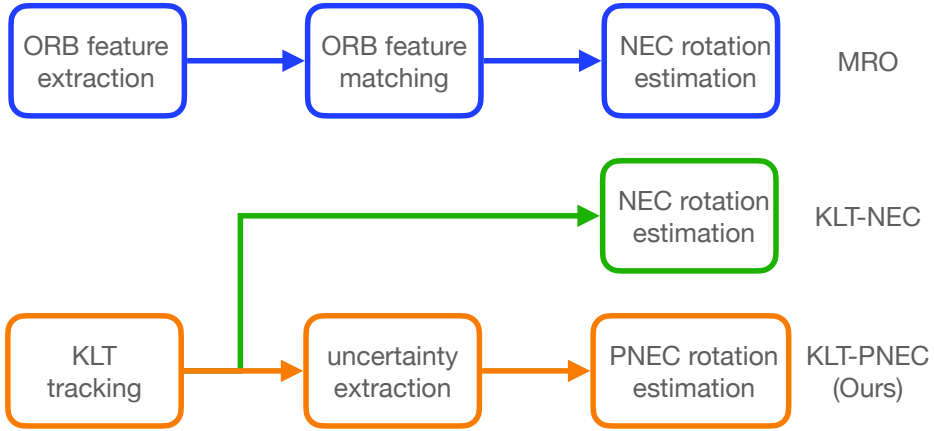

- C. Chng, Á. Parra, T. Chin, and Y. Latif. Monocular rotational odometry with incremental rotation averaging and loop closure. Digital Image Computing:Techniques and Applications (DICTA), 2020.

Evaluation

KITTI Odometry Dataset

	MRO		KLT-NEC		KLT-PNEC (Ours)	
Seq.	RPE_1	RPE_n	RPE_1	RPE_n	RPE_1	RPE_n
00	0.36	8.67	0.127	4.935	**0.121**	**4.706**
01*	**0.29**	**16.03**	0.692	25.548	0.853	27.783
02	0.29	16.03	**0.087**	**5.876**	0.101	6.010
03	0.28	5.47	**0.056**	2.453	0.060	**1.410**
04	0.04	1.08	0.042	0.792	**0.038**	**0.531**
05	0.25	11.36	0.085	4.641	**0.056**	**2.746**
06	0.18	4.72	0.144	4.443	**0.081**	**2.967**
07	0.28	7.49	0.074	5.207	**0.070**	**2.149**
08	0.27	9.21	0.063	5.593	**0.056**	**2.909**
09	0.28	9.85	0.104	**3.526**	**0.081**	3.866
10	0.38	13.25	0.086	5.094	**0.071**	**4.012**

Table: * In seq. 01 the KLT implementation fails and produces many wrong tracks due to self-similar structure. Since neither tracks nor covariances are correct, we omit this sequence in the ablation study.

Evaluation

KITTI Odometry Dataset

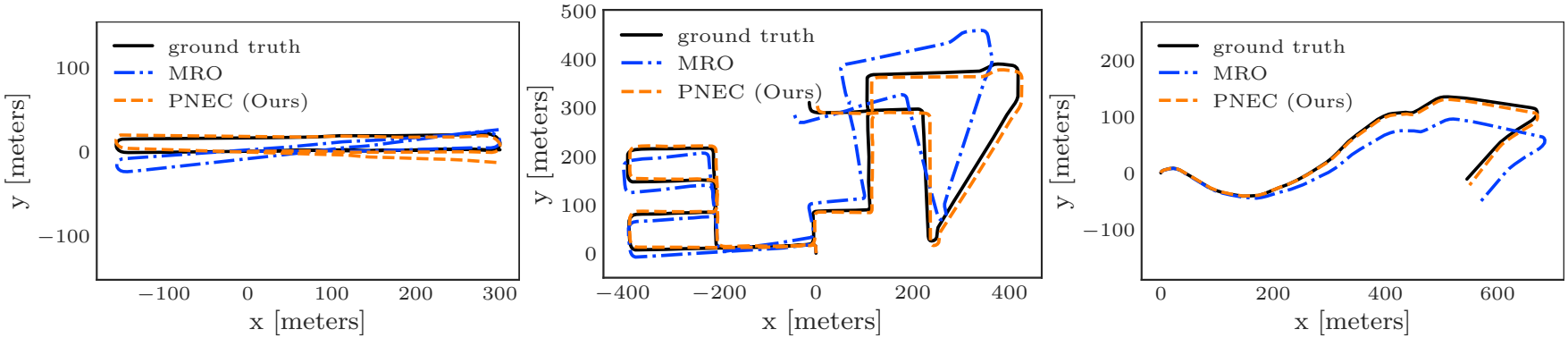

Figure: Trajectory generate from rotation estimations on seq. 06, seq. 08, and seq. 10

Evaluation

Ablation Study

	OMNI		PINHOLE		KITTI	
Metric	e_{rot}	e_{rot}	e_{rot}	e_{rot}	RPE_1	RPE_n
Noise level [px]	1.0	3.0	1.0	3.0		
NEC	0.143	0.240	0.313	0.537	0.087	4.256
PNEC w/o LS	0.120	0.206	0.272	0.472	0.074	4.088
PNEC only LS	**0.108**	**0.191**	**0.252**	**0.439**	0.140	5.523
PNEC (Ours)	0.114	0.199	0.262	0.459	**0.073**	**3.131**

Table: Ablation study on synthetic data and the KITTI dataset (averaged results)

Evaluation

Runtime

	MRO	KLT-NEC	KLT-PNEC
feature creation	36	23	23
matching	120		
optimization	5	33	54
total time (ms)	161	56	77

Table: Runtime study on the KITTI dataset. PNEC achieves real-time performance.

Rotation Estimation under Uncertain Feature Positions

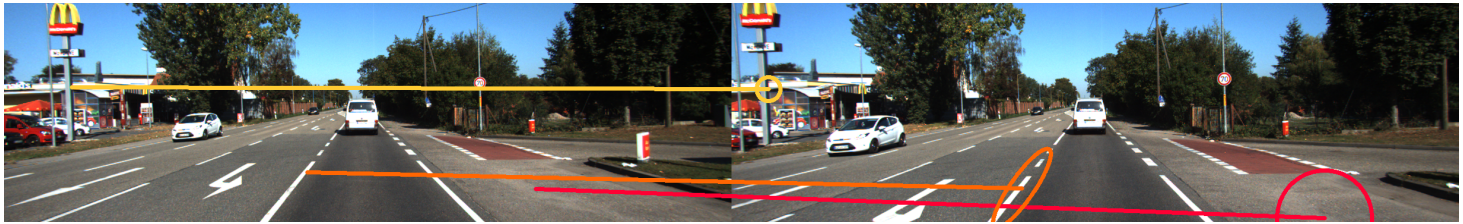

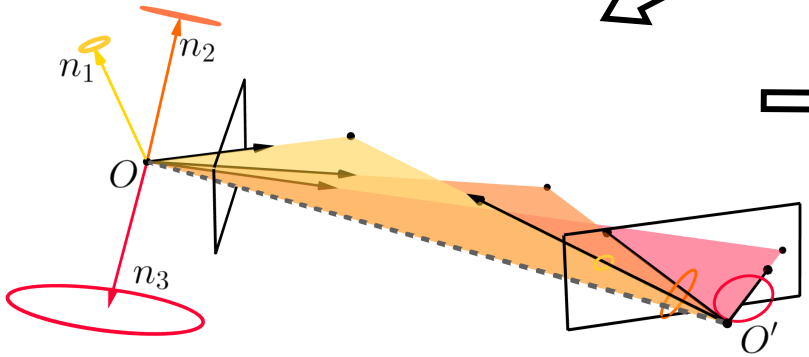

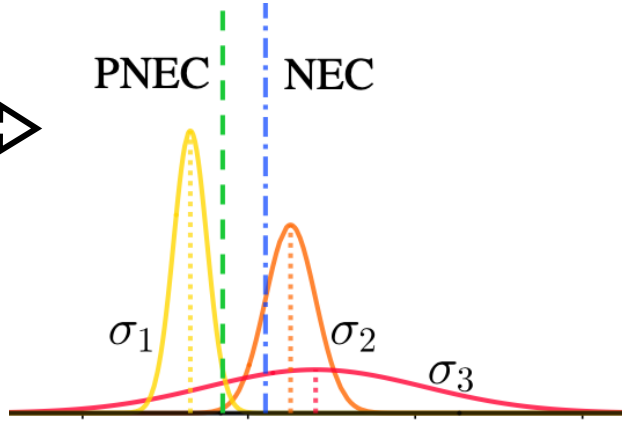

Backup

SCF

Iterative algorithm for the optimization over $\boldsymbol{t}$

$$E_P(\boldsymbol{R},\boldsymbol{t}) = \sum_i \frac{\boldsymbol{t}^\top \boldsymbol{A}_i \boldsymbol{t}}{\boldsymbol{t}^\top \boldsymbol{B}_i \boldsymbol{t}} + \boldsymbol{t}^\top \boldsymbol{D} \boldsymbol{t}\,, \tag{14}$$

with

$$\begin{aligned} \boldsymbol{A}_i &= \hat{\boldsymbol{f}}_i \boldsymbol{R} \boldsymbol{f}'_i \boldsymbol{f}'^\top_i \boldsymbol{R}^\top \hat{\boldsymbol{f}}_i^\top\,, \\ \boldsymbol{B}_i &= \hat{\boldsymbol{f}}_i \boldsymbol{R} \boldsymbol{\Sigma}_i \boldsymbol{R}^\top \hat{\boldsymbol{f}}_i^\top + c\boldsymbol{I}_3\,, \\ \boldsymbol{D} &= \boldsymbol{0}\,. \end{aligned} \tag{15}$$

Compute the $\boldsymbol{E}$-matrix, a 3×3 symmetric matrix given by

$$\begin{aligned} \boldsymbol{E}(\boldsymbol{R},\boldsymbol{t}) &= \sum_i w_i \cdot \left(\boldsymbol{t}^\top \boldsymbol{B}_i \boldsymbol{t} \cdot \boldsymbol{A}_i - \boldsymbol{t}^\top \boldsymbol{A}_i \boldsymbol{t} \cdot \boldsymbol{B}_i \right)\,, \\ w_i &= (\boldsymbol{t}^\top \boldsymbol{B}_i \boldsymbol{t})^{-2} \cdot \prod_j \boldsymbol{t}^\top \boldsymbol{B}_j \boldsymbol{t}\,. \end{aligned} \tag{16}$$

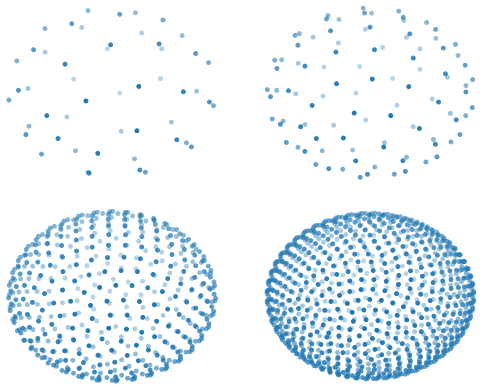

Figure: Fibonacci sampling on the unit sphere

Backup

Metrics

$$e_{rot} := \angle(\boldsymbol{R}^\top \tilde{\boldsymbol{R}}), \text{ and}$$
$$e_t := \arccos(\boldsymbol{t}^\top \tilde{\boldsymbol{t}}) \tag{17}$$

between the ground truth $\boldsymbol{R}, \boldsymbol{t}$ and the estimated values $\tilde{\boldsymbol{R}}, \tilde{\boldsymbol{t}}$, where $\angle(\cdot)$ returns the angle of the rotation matrix.

$$\mathrm{RMSE}(\Delta) := \left(\frac{1}{m} \sum_{i=1}^{m} E_i^2 \right)^{\frac{1}{2}} \tag{18}$$

over $m := n - \Delta$ residuals for frame pairs that are a “time-step" Δ apart.

$$E_i := \angle((\boldsymbol{R}_i^\top \boldsymbol{R}_{i+\Delta})^\top (\tilde{\boldsymbol{R}}_i^\top \tilde{\boldsymbol{R}}_{i+\Delta})) \tag{19}$$

between the ground truth $(\boldsymbol{R}_i^\top \boldsymbol{R}_{i+\Delta})$ and the estimated $(\tilde{\boldsymbol{R}}_i^\top \tilde{\boldsymbol{R}}_{i+\Delta})$ relative rotations.

$$\mathrm{RPE}_1 := (RMSE)(1) \tag{20}$$

$$\mathrm{RPE}_n := \frac{1}{n} \sum_{\Delta=1}^{n} \mathrm{RMSE}(\Delta) \tag{21}$$

Probabilistic Normal Epipolar Constraint

Dominik Muhle
Technische Universität München
Fakultät für Informatik
Chair of Computer Vision & Artificial Intelligence
München, 23. September 2021